

INDEX OF REFRACTION OF NICKEL AS A FUNCTION
OF TEMPERATURE

by

MILFORD RAY LEE

B. S., Kansas State College
of Agriculture and Applied Science, 1949

A THESIS

submitted in partial fulfillment of the

requirements for the degree

MASTER OF SCIENCE

Department of Physics

KANSAS STATE COLLEGE
OF AGRICULTURE AND APPLIED SCIENCE

1950

Docu-
ment
LO
2668
.74
1950
L44
c.2

TABLE OF CONTENTS

INTRODUCTION	1
EXPERIMENTAL APPARATUS AND PROCEDURE	7
The High Temperature Camera	7
Source of Monochromatic Radiation	14
Preparation of The Reflecting Surface	15
The Annealing and Outgassing Process	18
Temperature Regulation and Measurement	22
Data Analysis	27
EXPERIMENTAL RESULTS	33
ERRORS AND CONCLUSIONS	41
ACKNOWLEDGMENT	45
LITERATURE CITED	46

INTRODUCTION

At the time of the discovery of x-rays, reflection and refraction of ordinary light by various media had been widely investigated. These same phenomena had been observed in the infrared and ultraviolet regions, and since x-radiation was found to be of the same electromagnetic character it was thought that radiation of this wave length would exhibit somewhat the same characteristics.

However in his original examination of the properties of x-rays, Roentgen (33) was unsuccessful in all attempts to obtain either refraction by means of prisms of a variety of materials or to detect any difference between the behavior of the rays at a rough surface and a polished surface of any material. Although these and many other early direct tests for the index of refraction were unsuccessful, Stenstroam (40) found that for x-rays whose wave lengths are greater than about 3 angstroms, reflected from certain crystals, Bragg's law,

$$n\lambda = 2d \sin\theta,$$

where λ = wave length of the radiation,

d = lattice spacing of the reflecting planes,

θ = angle of reflection,

does not give accurately the angles of reflection. The difference was attributed to an appreciable refraction of the rays by the crystals.

Measurements by Duane, as noted in Compton and Allison (7),

and Siegbahn (35) have shown that discrepancies, though very small, occur when x-rays are reflected from calcite.

The direction of the deviations in Stenstrom's (40) experiments indicated that the index of refraction is less than 1. This being the case, total reflection should occur when x-rays in air strike a plane surface at a sufficiently sharp glancing angle. The condition for total reflection is that $\sin r = \frac{1}{\mu} \sin i$, where i = angle of incidence,
 r = angle of refraction,
 μ = index of refraction.

In this case the angle of refraction is imaginary, and all of the energy must be either reflected or absorbed. In terms of the glancing angle θ , which is the complement of the angle of incidence i , this may be written, to a first degree of approximation,

$$\theta^2 = 2(1 - \mu^2).$$

The quantity $(1 - \mu^2)$ is quite convenient to deal with rather than μ^2 itself, and is usually designated by the letter \mathcal{J} .

With this substitution the equation has the form,

$$\mathcal{J} = \frac{1}{2} \theta_c^2.$$

By measuring the critical angle for total reflection θ_c , the index of refraction can be determined.

Refractive indices were first measured in this way in 1922 by Compton, as cited in Compton and Allison (7), and since that time many others have used the same procedure. Table 1 lists the names of experimenters who have used the method of total reflection for the investigation of the indices of refraction of various substances.

Table 1. Experimenters who have used the total reflection method for investigating the index of refraction of x-rays.

Investigator	Substances Investigated
Carrara (5)	The common metals
Compton (7)	Crown glass
Davis and Terrill (8)	Calcite
Dersham (9,10)	Gold and silver
Doan (11)	Glass
Edwards (14)	Nickel
Gehman (18)	Aluminum
Kellermann (21)	Glass and silver
Kiessig (22)	Nickel
Kirkpatric (23)	Rock salt
Lashkareff and Hertzruecken (24)	Glass
Linnik and Lashkareff (25)	Quartz, glass and ice
Smith (37)	Water, glycerine and other liquids
Stauil (39)	Nickel
Thibaud (41)	Glass
Wolfers (47)	The common metals

The theoretical explanation of the index of refraction for electromagnetic waves was first deduced by Lorentz and Drude, according to Sproull (38), on the basis of classical physics. Their results were later applied to the x-ray region giving

$$D = \frac{e^2}{2\pi m} \sum \frac{n_q}{\nu^2 - \nu_q^2}$$

where e = charge on an electron in esu,

m = mass of an electron,

ν = frequency of the refracted ray,

ν_q = various natural frequencies of electrons in the refracting medium,

n_q = number of electrons per cubic centimeter of natural frequency ν_q .

It was found later, however, that the Lorentz theory is inadequate when the frequency of the refracted ray is quite close to a natural frequency present in the material. The present theory advanced by Hönig, as reproduced in Compton and Allison (7), was derived on the basis of quantum mechanics and is in fair agreement with experiment in the region of a natural absorption frequency. It was this theory which was used to check the values obtained in this experiment, and although the final expression is too cumbersome to be noted here it can be found in any standard advanced x-ray text, including "X-rays in Theory and Experiment", by A. H. Compton and S. K. Allison, pp. 311-312.

Although many total reflection experiments have been carried out at room temperature nothing could be found in the literature concerning the experimental variation of the index of refraction for x-rays as a function of temperature.

Theory predicts that α should be directly proportional to the density of the refracting material since the only quantity on the right of the above expression which is a function of the temperature is n , the total number of electrons per cubic centimeter.

The reason for undertaking this experiment was due to work recently done by Cardwell (4) on the photoelectric and thermionic properties of nickel which indicated that a slight change in reflected intensity should occur in the region of magnetic transformation. To detect such a change it was desirable to use as nearly monochromatic radiation as could be obtained. However, in so doing the exposure time was increased to a prohibitive length, and this phase of the experiment was abandoned. It is suggested that such a change in the reflected intensity, if it exists, might be detected with a precision spectrometer.

The fact that α is predicted to be directly proportional to the density of the refracting medium suggested the possibility of an independent evaluation of the linear coefficient of expansion of the material.

An anomaly in the linear coefficient of expansion of nickel was observed as early as 1905 by Randall (32) and verified 5 years later by Colby (6). The reason for the anomaly was ascribed to the disappearance of ferromagnetism from the metal.

The increase in volume due to ferromagnetism is accounted for roughly by the Heisenberg theory as shown by Fowler and Kapitza (16), but a quantitative explanation has not yet been

deduced. However, several investigators (27, 28, 45) have determined fairly consistent experimental values for the ferromagnetic change in length per unit length.

The temperature at which the metal no longer exhibits ferromagnetic properties is called the Curie point, and has been the subject of much investigation. Some of the experimenters who have investigated the Curie point of nickel since 1905 are listed in Table 2.

Table 2. Experimenters who have investigated the Curie point of nickel.

Investigator	Date
Randall (32)	1905
Colby (6)	1910
Hidnert (19)	1927
Gaponov (17)	1930
Powell (30)	1930
Simon and Gergmann (36)	1930
Uffelmann (42)	1930
Eucken and Dannohl (15)	1934
Williams (45)	1934
Procopiu and Farcas (31)	1935
Owen and Yates (28)	1936
Rosenbohm and Jaeger (34)	1936
Bryant and Webb (3)	1939
Nix and MacNair (27)	1941
Drigo and Pizzo (12)	1948
Cardwell (4)	1949

It was felt that a study of the index of refraction as a function of temperature might shed additional light on the expansion of nickel in the region of magnetic transformation.

EXPERIMENTAL APPARATUS AND PROCEDURE

The apparatus consisted essentially of a high temperature camera in which the sample was mounted, and a double crystal monochromator to select the desired wave length of radiation. The beam of x-rays emerging from the monochromator was reflected from the polished surface of the sample and recorded on a photographic plate. The index of refraction was then determined from the width of the recorded line.

The High Temperature Camera

The camera chamber proper was constructed of 8 inch diameter brass tubing, the depth being just sufficient to allow $\frac{1}{4}$ inch clearance between the top of the furnace and the water cooled cover plate. The base of the chamber was cut from $\frac{3}{8}$ inch brass stock for strength. A $\frac{3}{16}$ inch seat was cut in the base to insure the proper fit. The two parts were well tinned after which they were sweated together at a temperature sufficiently high to allow the soft solder to flow freely, thereby completing the vacuum seal at that joint.

The cover plate was made of $\frac{1}{4}$ inch brass plate, and since it was to be removable a double shoulder was cut in the underneath edge to give maximum seating surface with the top rim of the chamber tube. The rim of the chamber was offset to

EXPLANATION OF PLATE I

Photograph of the apparatus.

PLATE I



complete the fit.

In order to introduce a rotating shaft into the vacuum chamber it was necessary to mount a special gasket in the base. The conventional type Wilson seal (46) was used. This type seal holds a well lubricated annular rubber gasket through which the rotating part is introduced into the chamber. The high external pressure keeps the gasket pressed firmly against the shaft, and the vacuum fit is maintained.

The camera chamber was mounted on a 16 inch by 16 inch base provided with a leveling screw at each of the four corners as shown in Plate I. The chamber was insulated from the camera mounting with a $\frac{1}{4}$ inch transite disc to minimize heat transfer from the camera.

The table upon which the sample holder was mounted was made an integral part of the drive shaft. The position of the holder could be adjusted with respect to the table by means of three thumb screws, two of which can be seen in Plate II, Fig. 1. A small hole was drilled through the sample holder, and one of the same size was drilled to a depth of $\frac{1}{4}$ inch in the table to coincide with the axis of the drive shaft. The holder was slotted to receive the sample, and the side of the slot against which the reflecting face of the sample was butted was made to coincide with the diameter of the small hole. It was then possible to adjust the face of the sample to a position such that the axis of rotation was in the plane of the reflecting surface. To do this the table and holder were first removed from the camera, and a needle of the proper size was fitted

into the small aligning hole. The sample holder could then be adjusted by means of the three adjustment screws until a point was reached at which continued rotation of the table produced no lateral displacement of the aligning needle.

The specimen table was driven by an electric motor which turned 40 rpm. To cut down the rate of rotation a gear box with 200 to 3 ratio was introduced between the motor and the table shaft. The resulting turning speed was $3/5$ rpm. In order to make the sample oscillate through an angle slightly greater than the critical angle an arm held rigidly to the table shaft was made to ride on a cardioid cam mounted on the end of the gear box shaft. The arm was held against the cam by spring tension so that as the cam turned at a constant angular velocity the specimen holder was caused to oscillate. The angle turned through could be adjusted slightly by changing the length of the riding arm. The cam and gear box assembly is shown in Plate II, Fig. 1.

The film holder was supported by a telescoping metal stand sufficiently rigid to keep the film fixed with respect to the incident beam throughout the exposure, and the sample to film distance was fixed as follows: A hole just the size of the table shaft was drilled in a flat brass strip of about 110 cm length. The strip was then cut to a length such that the distance from the end of the strip to the center of the hole was accurately 100 cm. The hole in the strip was then slipped onto the table shaft and the film plate butted against the cut end of the strip. Since the center of the specimen holder could

EXPLANATION OF PLATE II

Fig. 1. Photograph showing the monochromator
and sample holder.

Fig. 2. Photograph showing the Geiger tube mounting.

PLATE II



Fig. 1



Fig. 2

be adjusted to a position directly above the center of the table shaft the distance from the sample to the film plate could be made the same as the distance from the center of the table shaft to the cut end of the brass strip, namely, 100 cm. The strip was supported by the right angle extrusion shown in Plate I. The final adjustment was the leveling of the brass strip by adjusting the height of the telescoping stand.

The cooling system consisted of six coils of $\frac{1}{4}$ inch copper tubing spaced around the circumference of the camera as shown, and, in addition, a short length of the same type tubing was used on the cover plate. Tap water at a temperature of roughly 16 degrees Centigrade was circulated through the system in amounts sufficient to keep the temperature of the camera within 2 or 3 degrees of input water temperature.

Source of Monochromatic Radiation

The radiation source was a cobalt target x-ray tube operated at 32 kv and a tube current of 10 ma. The radiation emerging from the tube head was first defined by a vertical lead slit and was incident upon the first crystal of a double crystal monochromator (Plate II, Fig. 1). The crystal was mounted on a small table free to rotate about a vertical axis, and which could be clamped in a fixed position by a lock nut. The table was rotated until the cleavage face made an angle θ with the incident beam, where θ is the Bragg angle for Cobalt K radiation and is the angle referred to in the equation on Page 1 of the introduction. With the first crystal in this position the K lines and the weak continuous radiation in the

same wave length range were reflected in the direction of the second crystal. This crystal also was mounted on a turntable, but the position adjustment was much more sensitive. The $K_{\alpha 1}$ and $K_{\alpha 2}$ lines, being of slightly different wave length, have different Bragg angles of reflection for a given reflecting plane. Therefore, if the second crystal could be rotated very slowly the two lines should be distinguishable by analyzing the radiation reflected from the monochromator unit.

This is what was done.

A Geiger tube was mounted to intercept the beam as shown in Plate II, Fig. 2. The relative intensity of the emergent beam was determined by noting the counting rate on the scalar shown in the right background of the same plate. It is well known that the $K_{\alpha 1}$ is more intense than the $K_{\alpha 2}$ line, so the two were easily distinguished by rotating the second crystal by means of a thumb screw until a maximum counting rate was observed.

To illustrate the resolution obtainable with this simple type monochromator, the difference in wave length of the $K_{\alpha 1}$ and the $K_{\alpha 2}$ lines of Cobalt is .0039 KX units, and is quite easy to pick off most any intensity between background and maximum of either line, so that peaking the instrument presented no problem.

The wave length of the Cobalt $K_{\alpha 1}$ line was taken to be 1.78529 KX units (7).

Preparation of the Reflection Surface

When reflecting x-rays at room temperature the usual procedure is to evaporate a film of the substance to be investigated onto a smooth glass or other suitable base. However, since this experiment was conducted over a temperature range of several hundred degrees, no such method could be employed. In order that no external mechanical stress be exerted on the crystals in the reflecting plane it was readily apparent that if the evaporation method were to be used the base could be of nickel only.

Correspondence with the International Nickel Company revealed that it would be possible to obtain a casting of Renzoni's type nickel of the required dimensions after a short delay. The impurities in this type nickel were listed as follows:

Co.	0.043 percent
Fe.	0.002 percent
Cu.	0.005 percent
Pb.	0.0008 percent

The purity exceeded expectations for a specimen of such volume, and a choice was available as to whether the evaporating or the polishing technic should be employed. The final decision was in favor of the latter for the following reasons:

1. High purity evaporation must be carried on a quite low pressure to avoid contamination of the sample.
2. Stauss (39) and others have found a variation in the critical angle with film thickness, and although several

investigators (39, 22, 14, 12, 45, 28) fail to agree on the reason for the variation, the discrepancy is real nevertheless.

3. Procopiu and Farcas (31) have found the Curie point to be 17 degrees higher than normal for nickel films of less than 40 microns thickness, and recent work by Drigo and Pizzo (12) has shown that certain magnetic properties of nickel films vary with film thickness.

4. The variation of the ferromagnetic properties of nickel with the percent of impurity has been well established (27, 28, 45).

5. Such effects as those listed above could be eliminated by using a polished face of the Renzoni's nickel block as the reflecting surface, the actual impurities in which were known.

The actual preparation of the sample was accomplished in the following way: The rough casting was first machined to the desired dimensions after which one face was turned down on a lathe until it was as plane and smooth as possible. The resulting surface, being extremely rough on a microscopic scale, was then worked down with cutting clothes of diminishing roughness. This phase of the polishing procedure was carried out on a surface plate to ensure continued planeness of the face. The process was repeated while using a mixture of alundum grit and alcohol as the abrasive. After several hours polishing with the finest grit (#600) available the smallest visible scratches heretofore present in the grinding process were eliminated. Under a microscope however the surface appeared to be quite rough. It remained to remove all pits due to the particle size of the grit. This was done on a lapping wheel using ferric oxide as the

polishing compound.

At frequent intervals during the final polishing process the sample was cleaned and mounted in the camera, and although it was found that the face need not be highly polished to reflect the rays, the exposure time necessary in the photographic recording of the reflection varied markedly with the roughness of the reflecting surface. Continued polishing resulted in the removal of a large majority of the pits from the surface with corresponding decrease in the necessary exposure time.

Although the reflecting surface need not be absolutely plane it is desirable that there be few points on the surface at which double reflection can occur. With this in mind the finished surface was checked with a Bausch and Lomb optical flat with sodium light. The resulting interference fringes were straight lines in the central part of the polished face.

The Annealing and Outgassing Process

After the polishing was completed the surface was an efficient reflector, but it was still unsuitable for a quantitative investigation of the critical angle of reflection.

When a metal is cold worked the natural orientation of the minute crystals comprising the metal is disturbed. The nature of the resulting change in orientation depends upon the metal, the type of cold work to which the metal is subjected, and the temperature at which the working takes place. There are other factors involved, but the ones noted are apparently the most significant.

The nature of the preferred orientation produced by cold work in the case of face centered cubic metals such as nickel has been studied by Polanyi and Weissenberg (29), Wever and Schmidt (44),,and others. However, the concern was not so much with the nature of the preferred orientation after working, but rather with devising a means of causing the crystals comprising the reflecting face to return to their natural unstrained condition. A careful annealing process was employed.

Before mounting the sample in the furnace the whole specimen was thoroughly cleaned to remove all trace of the materials used in the polishing process. The furnace was mounted in the camera and the chamber evacuated to a pressure of approximately 10^{-3} mm of hg before beginning the heating process.

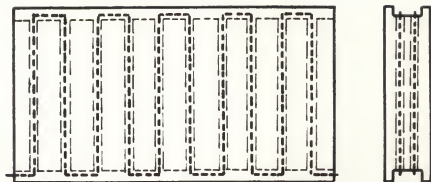
The temperature of the sample was raised slowly at first until the pressure of the system was reduced sufficiently to prevent oxidation of the polished face. The furnace was then raised to a temperature of 380 degrees Centigrade and allowed to cool slowly. When the sample had reached a point well below the transformation temperature, the temperature of the furnace was again raised and the process repeated.

At regular intervals the sample was exposed to the x-ray beam to determine the extent of reorientation of the crystals in the reflecting plane. After a treatment period of 600 hours the sample was sufficiently annealed and outgassed to give consistent readings. The apparatus was then disassembled and the specimen removed to examine the surface for traces of

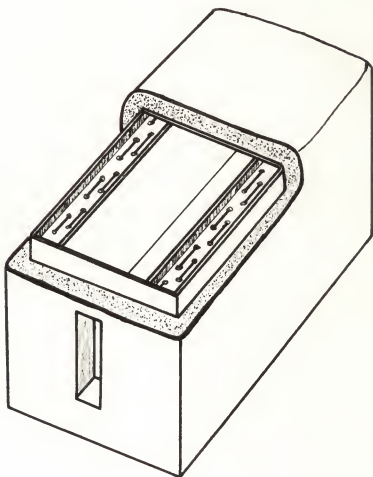
EXPLANATION OF PLATE III

Drawing of the principal parts of the furnace.
View A shows a side and an end view of the heater plates. The dashed lines indicate the position of the windings. The relative spacing of the two filament windings is shown in View B.

PLATE III



A



B

oxidation. None could be detected.

The peak temperature of 380 degrees Centigrade was chosen after Owen and Yates (28) who found no oxidation occurring with a nickel sample at a pressure of 10^{-3} mm of hg and a temperature of 400 degrees Centigrade.

Temperature Regulation and Measurement

In building the furnace the prime consideration was to employ a design which would maintain as nearly as possible a constant temperature throughout the interior of the enclosure. Plate III shows the major parts of the design selected.

The heating plates were constructed from $\frac{1}{2}$ inch brass stock, and the holes, drilled vertically through the plates, were made just large enough to allow room for the small procelain insulating beads which were strung along the full lengths of the heater windings. The ends and the top of the furnace were made of $\frac{1}{8}$ inch brass plate, and the parts were assembled with brass screws.

Both the coarse and the fine adjustment filaments were of No. 24 nichrome wire of roughly 120 cm length. The voltage range of the coarse adjustment was 0 to 115 volts, whereas the range of the fine adjustment winding was from 0 to 24 volts. Voltage regulation was attained by means of a General Electric 0.750 kva voltage stabilizer.

A schematic diagram of the control circuit is shown in Plate IV.

EXPLANATION OF PLATE IV

Schematic wiring diagram of the furnace control circuit.

A - ammeter.

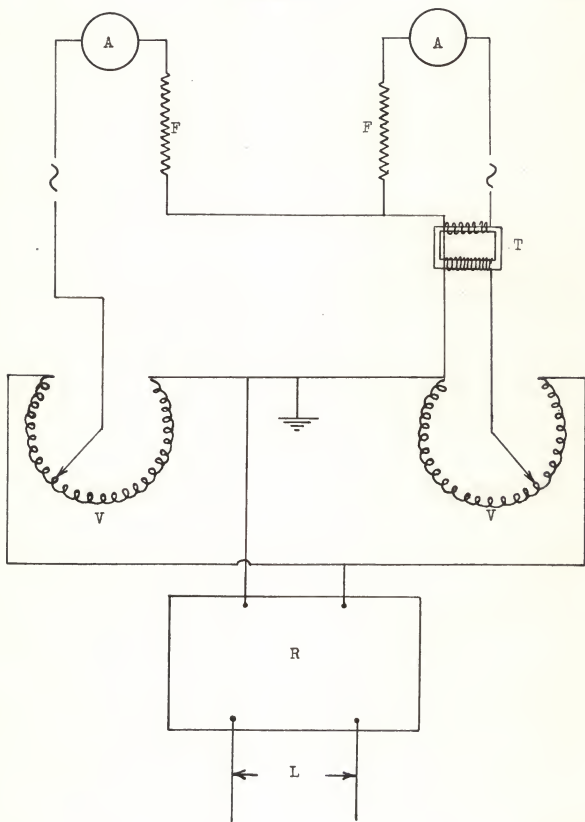
F - filament.

T - step-down transformer.

V - variac.

R - voltage regulator.

L - 115 volt A.C. line.



After the unit was completely assembled a $3/8$ inch jacket of asbestos putty was applied leaving only the windows and the bottom open. It was necessary to apply the putty in layers of about $1/8$ inch thickness and allow each layer to dry before applying the next. This procedure prevented the putty from shrinking away from the metal surfaces as it dried, and an even insulating jacket was obtained.

The bottom of the furnace was left open in order that it could be removed from the camera without disturbing the setting of the sample. In order to obtain the proper insulation below the sample, the entire specimen table was covered with a thick coating of asbestos. The base of the sample holder was grooved to hold the furnace rigidly in place as well as to complete the insulation about the base of the heating plates.

The completed furnace is visible in the upper background of Plate II, Fig. 1.

Three chromel-alumel thermocouples were used to determine the temperature distribution throughout the sample. It can be noted in Plate II, Fig. 1, that one of the three was placed directly in the center of the block, and the other two were placed approximately $1/4$ inch from the top and side edges. The junctions were buried to within $1/16$ inch of the reflecting surface. Since the specimen was symmetrical about the center thermocouple the temperature gradient throughout the sample could be roughly determined by noting the readings of each of the three thermocouples at a given time. A typical record of these data is reproduced in Table 3.

Table 3. Thermocouple data.

Film number :	Thermocouple readings in mv :			Time	Date
	#1 (outer):	#2 (upper):	#3 (center):		
91	14.73	14.76	14.88	09:10	4/8/50
	14.73	14.77	14.89	09:30	
	14.79	14.82	14.94	10:30	
	14.78	14.80	14.93	11:00	
	14.75	14.78	14.91	11:30	
	14.75	14.77	14.89	12:30	
	14.73	14.76	14.86	17:30	
	14.73	14.76	14.87	21:10	

The magnitude of the emf produced in each couple was determined by means of a Leeds and Northrup Type K-2 potentiometer, and the corresponding temperatures were obtained by referring to a standard chromel vs. alumel thermocouple chart (43).

The corrected temperature of the portion of the reflecting face used was determined as follows: The difference in temperature registered by the central thermocouple and the one lying in the same horizontal plane, (No. 1), was, on the average, no greater than 4 degrees, and the distance between the two was approximately 3 cm. The divergence of the beam from the second crystal was approximately 6 seconds or 3×10^{-5} radians of arc, and the glancing angle between the beam and the sample at the critical angle was about 7.5×10^{-3} radians. A short calculation showed that the portion of the reflector bathed by the beam under these conditions was less than 0.8 mm in width which was scarcely more than the width of the thermocouple junction buried immediately behind the point of reflection. It was seen that the temperature gradient in the horizontal direction could be neglected.

The reading of thermocouple No. 2, since its hot junction was in the area bathed by the beam, had to be considered in the determination of the corrected temperature. It can be noted in Table 3 that the maximum difference in emf registered by No. 2 and No. 3 was 0.13 mv. This corresponds to a temperature difference of 3.25 degrees at a sample temperature of about 365 degrees Centigrade. In view of the fact that the temperature regulation was no better than ± 2 degrees the average of the two readings was taken as the representative emf developed.

The mean value of emf registered by each thermocouple during an exposure was obtained from the expression,

$$T_m = \left\{ \frac{T_1 t_1}{t_1} \right.$$

where T_m = mean thermocouple emf,

T_1 = average of the i-th and i-th + 1 thermocouple reading,

t_1 = time interval between the i-th and i-th + 1 thermocouple reading.

Data Analysis

In the course of preliminary observations it was noted that the width of the reflected beam varied somewhat with exposure time, and in addition, the cutoff edge became increasingly diffuse as the length of exposure time was increased beyond a certain point. The broadening was caused by exposing the film above its linear region, which resulted in a flattening of the peak of the densitometer trace. The increased diffuseness of the cutoff edge was apparently due to the accumulative effect

EXPLANATION OF PLATE V

Photograph of a series of exposures showing the effects of over exposure, air scattering and incomplete annealing of the sample.

A-48 hour exposure with incompletely annealed sample.

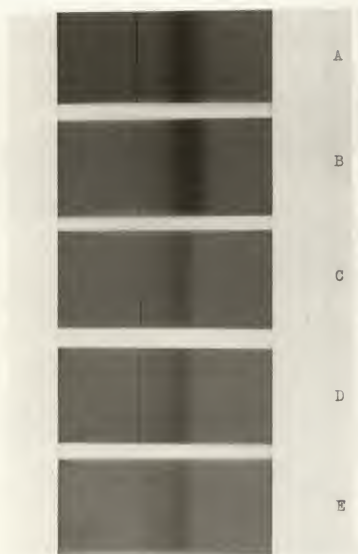
B-40 hour exposure with incompletely annealed sample.

C-Sample annealed. 24 hour exposure.

D-Sample annealed. 18 hour exposure.

E-Sample annealed. 12 hour exposure.

PLATE V



of air scattering over the long exposure. As a result the exposure time was reduced to a point which would cause just enough blackening to give a good densitometer trace. Plate V illustrates the above effects.

The typical micro-densitometer trace reproduced in Plate VI shows the variation in intensity of the reflected beam at the cutoff edge, and as predicted by H \ddot{u} nl, stated in Compton and Allison (7), there is no complete discontinuity in reflection at that point. It was for this reason that the width of the reflected beam was determined from the densitometer trace rather than by direct measurement of the blackened film.

The point of half maximum on the cutoff edge of the curve was chosen as representative of the cutoff position, and the height of half maximum was established as follows: The densitometer was first adjusted to make the recording pen coincide with the ∞ (infinity) position on the semi-logarithmic recording paper when there was total blackening of the film. Since the ordinate of the recording paper was plotted on the logarithmic scale, the values of B_m and B_b could be read directly from the graph, and $B_{\frac{1}{2}}$ was deduced from the expression,

$$B_{\frac{1}{2}} = \frac{1}{2}(B_m + B_b)$$

where $B_{\frac{1}{2}}$ = height of half maximum blackening,

B_m = height of maximum blackening or the peak of the smooth curve,

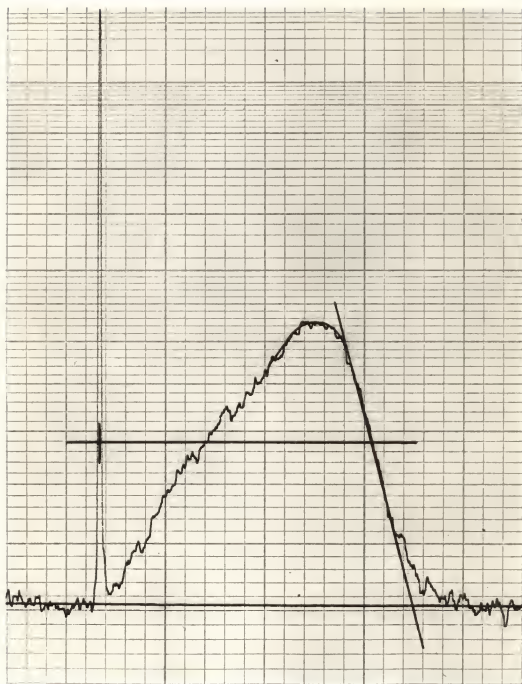
B_b = height of the background blackening.

The position of maximum blackening was determined by drawing a smooth peak through the trace, and the background was established by drawing a straight line through the indicated background as

EXPLANATION OF PLATE VI

Typical micro-densitometer trace showing the method of analysis. The sharp line on the left is the unreflected reference line. The cutoff edge is on the right.

PLATE VI



shown in Plate VI. The horizontal distance from the center of the reference line to the point of half maximum was then proportional to the width of the reflected beam. The final determination of the width was made on the micro-comparator.

It is to be noted that the densitometer trace does not indicate the relative reflected intensities from the reference line to cutoff. The drive cam was designed so that the sample swept through an angle slightly less than the critical angle in a short time, and then moved across the critical angle quite slowly. In this way the total exposure time necessary was reduced considerably since for a large fraction of the total time the sample was reflecting in the neighborhood of the cutoff edge.

Each film was processed in exactly the same way as follows:

Exposure time	12 hours
Time in developer	5 minutes
Time in fixing solution	10 minutes
Time in wash	30 minutes

The temperature of the processing solutions was maintained at 16 degrees Centigrade. Film from the same package was used throughout the experiment, and the shrinkage correction amounted to 0.2 percent. The shrinkage was assumed to be the same in each film.

EXPERIMENTAL RESULTS

Determinations of the widths of the reflected beam, S_t , were made through a temperature range of 20 degrees Centigrade, to 535 degrees Centigrade, although the values of S for

temperatures above 395 degrees Centigrade were discarded because of the indicated oxidation of the sample.

Since \mathcal{J} is proportional to S^2 , the values of \mathcal{J} were not computed for the entire temperature range, but the values of S^2 were obtained instead. From the proportionality of S^2 and it is seen that $\frac{\mathcal{J}_0}{\mathcal{J}_t} = \frac{S_0^2}{S_t^2}$ where the value of S_t^2 at 0 degrees Centigrade was obtained by plotting S^2 vs. temperature and extrapolating the curve back to 0 degrees Centigrade. The values obtained are listed in Table 4. When the last significant figure of an entry is in doubt, it is listed as a subscript.

An attempt was made to observe the reported thermal hysteresis in the Curie point at low pressure (34), but none was observed.

A plot of $(\frac{\mathcal{J}}{\mathcal{J}_0} - 1) \times 10^3$ vs. temperature is shown in the upper left hand corner of the graph in Plate VII. The values in the region from 300 degrees Centigrade to 400 degrees Centigrade were plotted on an enlarged scale in order to determine more specifically the nature of the change of slope of the curve in the region of magnetic transformation. The original plot was made on 24 inches paper.

Although there is a definite change in slope between 350 degrees Centigrade and 360 degrees Centigrade the exact nature of the change is in considerable doubt. The plot in Plate VII indicates one possible fit to the points obtained.

If \mathcal{J} is directly proportional to the density as predicted then the slope of the above mentioned curve should be three

Table 4. Film data. $S_0 = 1.544_0$ $s_0^2 = 2.384_0$

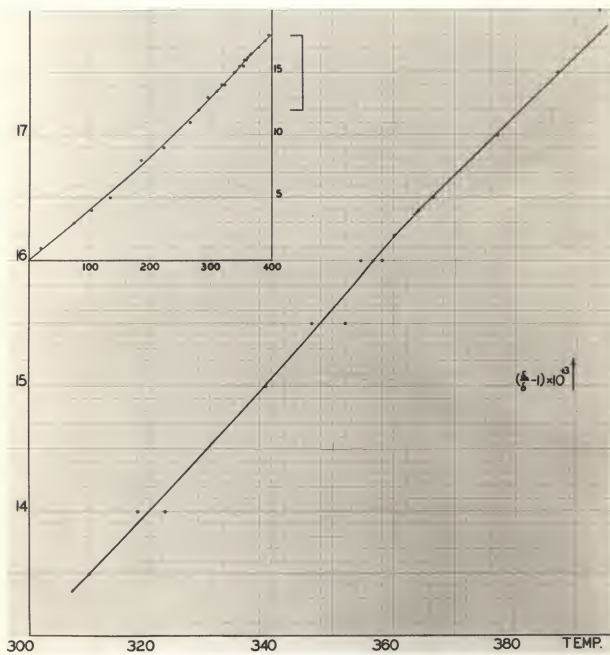
Film no. :	Temperature :	S :	s^2 :	$\frac{d_0}{d}$
97	20	1.543 ₀	2.381 ₀	1.001 ₀
94	76	1.541 ₅	2.376 ₂	1.003 ₀
71	104	1.541 ₀	2.374 ₆	1.004 ₀
93	135	1.540 ₀	2.372 ₁	1.005 ₀
77	185	1.538 ₀	2.365 ₄	1.008 ₀
76	222.5	1.537 ₀	2.362 ₇	1.009 ₀
78	266	1.535 ₅	2.357 ₈	1.011 ₀
62	280	1.535 ₀	2.356 ₂	1.012 ₀
79	295	1.534 ₀	2.353 ₁	1.013 ₀
80	310	1.533 ₇	2.352 ₂	1.013 ₅
81, 69	318	1.533 ₃	2.351 ₀	1.014 ₀
82, 67	322.5	1.533 ₃	2.351 ₀	1.014 ₀
83, 72	339	1.532 ₆	2.348 ₇	1.015
73	346.5	1.532 ₂	2.347 ₆	1.015 ₅
84	352.5	1.532 ₂	2.347 ₆	1.015 ₅
74	354.5	1.531 ₈	2.346 ₄	1.016 ₀
92	356	1.531 ₈	2.346 ₄	1.016 ₀
63	358	1.531 ₈	2.346 ₄	1.016 ₀
75	360	1.531 ₆	2.345 ₉	1.016 ₂
85	364.5	1.531 ₅	2.345 ₅	1.016 ₄
90	366.5	1.531 ₄	2.345 ₃	1.016 ₅
86, 89	377	1.531 ₀	2.344 ₁	1.017 ₀
87	387	1.530 ₅	2.342 ₇	1.017 ₅
88	395	1.530 ₀	2.341 ₉	1.018 ₀

EXPLANATION OF PLATE VII

$(\frac{d\alpha}{J} - 1) \times 10^3$ is plotted as a function of temperature for the range 0 degrees Centigrade to 400 degrees Centigrade as shown in the upper left of the plate. The region from 300 degrees to 400 degrees is shown on an expanded scale in the main part of the graph.

The slope of this curve is three times the linear coefficient of expansion. An anomaly can be seen in the slope in the temperature range from 350 degrees to 370 degrees Centigrade.

PLATE VII



EXPLANATION OF PLATE VIII

The curve shows a plot of $\alpha \times 10^6$ vs. temperature in degrees Centigrade where α is the linear coefficient of expansion in cm^{-1} . The values for this plot were obtained directly from the curve in Plate VII.

The base line is Gruneisen's theoretical curve obtained from the equation

$$\alpha = \frac{C_V}{3Q_0} \left[1 - \frac{m+n+3}{6} \frac{E}{Q_0} \right]^2$$

where $E = \int_0^T C_V dT$

$$Q_0 = V_0 / \gamma K_0$$

K_0 = compressibility,

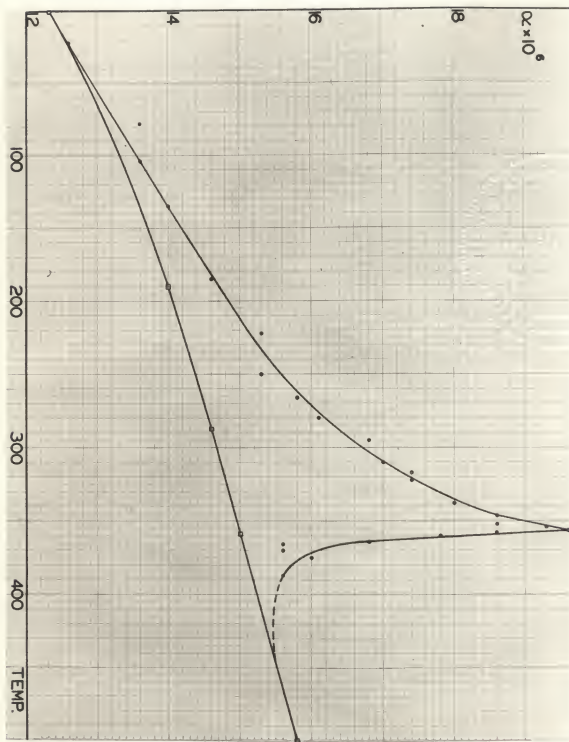
V_0 = atomic volume,

γ = Gruneisen's constant,

C_V = specific heat, and m and n are the exponents of the attractive and repulsive terms relating energy to the distance between vibrating atoms in a monatomic solid.

These values were taken directly from work done by Nix and MacNair (27).

PLATE VIII



times the linear coefficient of expansion, α , for

$$\frac{\rho_0}{\rho_t} = (1 + 3\alpha t) = \frac{f_0}{f}$$

where ρ_0 is the density at 0 degrees Centigrade, and ρ_t is the density at t degrees Centigrade.

The assumption that the volumetric coefficient of expansion is equal to 3α can be justified for a crystal of the cubic type.

Values of the slope were taken directly from the plot in Plate VII, and the values obtained for α were plotted as a function of temperature as shown in Plate VIII. The anomalous increase in volume appears to begin in the vicinity of room temperature reaching a maximum around 350 degrees Centigrade, after which there is a sharp decrease toward the theoretical value.

It must be noted that once the curve in Plate VII is drawn the plot of α vs. temperature is determined. As was stated, there is considerable doubt as to the best fit to the points plotted in the graph of $(\frac{f_0}{f} - 1) \times 10^3$ vs. temperature, so that the plot of α vs. temperature may be taken only as a general indication of the anomalous change. The area under this curve gives the change in ferromagnetic length per unit length, and this area was determined to check the experimental values obtained as to order of magnitude.

The area was found to be 4.0×10^{-4} .

Values of previous determinations of $\frac{\Delta l}{l}$ are listed in Table 5.

Table 5. Experimental values of the change in ferromagnetic length per unit length for high purity nickel.

$\frac{dL}{L}$	Purity of sample	Experimenter
3.65×10^{-4}	99.90 percent	Nix and MacNair (27)
2.4×10^{-4}	99.98 percent	Owen and Yates (28)
0.92×10^{-4}	99.85 percent	Williams (45)

The value for \int at room temperature was found to be 29.8×10^{-6} as compared with the theoretical value obtained from Hbnl's formula of 32.8×10^{-6} . The experimental value is in good agreement with that reported by Kiessig (22).

ERRORS AND CONCLUSIONS

The experimental determination of \int as a function of temperature was accomplished by the evaluation of only three quantities. These quantities are listed below.

1. The temperature of the sample.
2. The distance from the reflector to the film plate.
3. The width of the blackened area of the film.

In the discussion of temperature measurement it was stated that the regulation was no better than ± 2 degrees Centigrade. Since no attempt was made to determine the exact point of magnetic transformation, if such a point exists, this was not a serious limitation.

The distance from the point of reflection to the film plate was established as described in the discussion of the high

temperature camera, and the error introduced into the final results due to the possible error involved in fixing this distance can be shown to be small. The length of the brass strip which determined the distance from the center of the sample table shaft to the film plate was determined by the use of the micro-comparator to be $100,000 \pm .005$ cm. However, an error of $\pm .01$ cm was introduced by the degree of precision to which the centering hole for the aligning needle could be drilled. The adjustment of the film plate to a position 90 degrees to the horizontal caused some difficulty. This was done with high grade steel blocks commercially machined to 90 degrees, but whose size permitted the alignment to be checked to a height of only $2\frac{1}{2}$ inches above the brass strip. Since the film was mounted at a point $\frac{1}{4}$ inches above the strip, an error quite possibly was introduced. The magnitude of the error was determined to be of the order of ± 05 cm. The thickness of the film envelope was taken into account by placing against the film plate a piece of film and one thickness of the paper used in making the envelope. The plate was then butted against the cut end of the brass strip and clamped in place. This made the emulsion of the film coincide with the 100 cm position. In order that the film clamps should not interfere with the beam they were placed at positions a few cm to each side of the point where the beam was intercepted by the film. In view of this an error of no more than 0.03 cm may have been introduced due to a slight buckling of the film inside the envelope. The total error appeared to be of the

order of 0.1 cm.

From the expression $\theta = \frac{S}{2D}$ it follows that $\frac{\Delta S}{S} = \frac{\Delta D}{D}$ since θ_c is independent of the distance to the film plate D. The above proportionality gives the value for $\frac{\Delta S}{S}$ to be .001, and although the value of S itself could be determined to better than 0.1 percent the relative change in S was not affected appreciably since the same D value was used throughout the experiment.

The evaluation of the third quantity, S, was considerably more critical than the determination of either the temperature of the sample or the specimen to film distance. It can be noted in Table 4 that the S values were carried to 4 places after the decimal with the last place being in doubt. Third place accuracy could be accomplished by means of the vernier scale on the micro-comparator, but the next place was estimated, with a large number of such readings being averaged to obtain the final approximation. Taking into account the possible error involved in the micro-densitometer drive calibration, the S values could be considered significant to no better than ± 0.0002 cm. This may have introduced a serious error in the values of S, and although these values were plotted in the graph of Plate VII as calculated, they are subject to significant error and only general conclusions can be drawn from the plot.

From the data obtained in this experiment the following conclusions were reached:

1. The value of \mathcal{J} for high purity nickel at room temperature is $(29.8 \pm .2) \times 10^{-6}$.

2. \mathcal{J} for nickel varies directly as the density to a first approximation.

3. A modification of the method employed could be used to obtain quantitative data concerning the anomalous change in volume of nickel in the region of magnetic transformation. The modifications suggested are the use of a precision spectrometer to obtain the critical angles and additional pumping apparatus to reduce the pressure in the camera.

ACKNOWLEDGMENT

Appreciation is expressed to Professor R. D. Dragsdorf under whose guidance this work was done, for his excellent advice and helpful criticisms throughout the experiment and the preparation of this manuscript. Appreciation is also expressed to E. M. Wise and the International Nickel Company for supplying the high purity nickel, and to Professor E. V. Floyd and Mr. D. A. Rittis for their assistance in the construction of the apparatus.

LITERATURE CITED

- (1) Aoyama, S., and T. Ito
Thermal expansion of nickel-copper alloys at low temperatures. Repts. Tohoku Imp. Univ. 27: 348-364. 1939.
- (2) Barrett, C. S.
Structure of metals. New York: McGraw-Hill Book Co. 1943.
- (3) Bryant, J. M., and J. S. Webb
Determination of the Curie point temperature by the high frequency resistance method. Rev. Sci. Instr. 10: 47-48. 1939.
- (4) Cardwell, A. B.
Photoelectric and thermionic properties of nickel. Phys. Rev. 76: 125-127. 1949.
- (5) Carrara, N.
On total reflection. Cimento 1: 107-114. 1924.
- (6) Colby, W. F.
Coefficient of expansion of nickel near its critical temperature. Phys. Rev. 30: 506-521. 1910.
- (7) Compton, A. H., and S. K. Allison
X-rays in theory and experiment. New York: D. Van Nostrand Co. 1935.
- (8) Davis, B., and H. M. Terrill
Refraction of x-rays in calcite. Natl. Acad. Sci. Proc., U.S.A. 8: 357-361. 1922.
- (9) Dershem, E.
Refractive indices of silver. Phys. Rev. 31: 1117. 1928.
- (10) _____
The index of refraction and absorption coefficient of gold for the K line of carbon. Phys. Rev. 35: 128. 1930.
- (11) Doan, R. L.
Refraction of x-rays by the method of total reflection. Phil. Mag. 4: 100-110. 1926.
- (12) Drigo, A., and M. Pizzo
Magnetization of thin ferromagnetic films. Nuovo cimento 5: 196-206. 1948.

- (13) Duane, W., and R. A. Patterson
On the x-ray spectra of tungsten. Phys. Rev. 16:
526-539. 1920.
- (14) Edwards, H. W.
Total reflection of x-rays from nickel films of various
thicknesses. Phys. Rev. 32: 712-714. 1928.
- (15) Eucken, A., and W. Danneohl
The thermal expansion of some alkali halides and
metals at high temperatures. Z Elektrochem. 40:
814-821. 1934.
- (16) Fowler, R. H., and P. Kapitza
Magnetostriction and the phenomena of the Curie point.
Proc. Roy. Soc. 124: 1-15. 1929.
- (17) Gaponov, V. I.
Effect of mechanical deformation on the Curie point
of nickel. Elektrotekh, (Moscow) 2-3: 29-30. 1930.
- (18) Gehman, S. D., and C. B. Bazzoni
Reflection of soft x-rays from aluminum. Phys. Rev.
31: 1117. 1928.
- (19) Hidnert, P., and W. T. Sweeney
Thermal expansion of some nickel steels. Phys. Rev.
29: 911. 1927.
- (20) James, R. W.
The optical principles of the diffraction of x-rays.
London: G. Bell and Sons. 1948.
- (21) Kellermann, K.
Refractive index of various substances for x-rays.
Ann. Phys. 4: 185-214. 1930.
- (22) Klessig, H.
Interference of x-rays on thin nickel films.
Naturwissenschaften 18: 847-848. 1930.
- (23) Kirkpatrick, P.
An experimental check of the optical theory of x-ray
reflection. Phys. Rev. 22: 414-419. 1924.
- (24) Laschkarew, W. E., and S. D. Hertzruecken
Eine verbesserung des totalreflektometers für
Röntgenstrahlen. Z. Phys. 52: 739-742. 1928.

- (25) Linnik, W., and W. Laschkarew
Die bestimmung des brechungsindex der rontgenstrahlen
aus der erscheinung der totalreflexion. Ztschr. f.
Phys. 38: 659. 1926.
- (26) McKeehan, L. W.
The crystal structure of iron-nickel alloys. Phys.
Rev. 21: 402-407. 1923.
- (27) Nix, F. C., and D. MacNair
Thermal expansion of pure metals. Phys. Rev. 69:
597-605. 1941.
- (28) Owen, E. A., and E. L. Yates
X-ray measurement of the thermal expansion of pure
nickel. Phil. Mag. 21: 809-819. 1936.
- (29) Polanyi, M., and K. Weissenberg
Das rontgen-faser diagramm. Ztschr. f. Phys. 9:
123-130. 1922.
- (30) Powell, F. C.
Direction of magnetization of single ferromagnetic
crystals. Proc. Roy. Soc. A130: 167-181. 1930.
- (31) Procopiu, S., and T. Farcas
Curie point variation in thin films. Ann. Sci. Univ.
Jassy 20: 75-82. 1935.
- (32) Randall, H. M.
Coefficient of expansion of nickel at its critical
temperature. Phys. Rev. 20: 85-88. 1905.
- (33) Roentgen, W. C.
On properties of x-rays. Ann. Physik 64, 1898.
- (34) Rosenbohm, E., and F. M. Jaeger
Localization of the transition points of allotropic
metals. Proc. Acad. Sci. Amsterdam 39: 366-374. 1936.
- (35) Siegbahn, M.
New precision instruments in the x-ray spectrum.
Comptes Rendus 173: 1350. 1921.
- (36) Simon, F., and R. Bergmann
Measurement of the thermal expansion in the anomalous
region. Z. Physik Chem. B 8: 255-280. 1930.
- (37) Smith, S. W.
The refractive index of liquids of x-rays. Phys. Rev.
40: 156-164. 1932.

- (38) Sproull, W. T.
X-rays in practice. New York: McGraw-Hill Book Co.
1946.
- (39) Stauss, H. E.
Reflection from plane surfaces. Phys. Rev. 34:
712-714. 1929.
- (40) Stenstroem, W.
Dissertation, Lund. 1919.
- (41) Thibaud, J.
Reflection of x-rays of long wave length by plane
mirrors, J. de Physique et de Radium 10: 137-148.
1930.
- (42) Uffelmann, F. L.
Expansion of metals at high temperature. Phil. Mag.
10: 633-659. 1930.
- (43) Weber, R. L.
Temperature measurements. Ann Arbor: Edwards Brothers.
1941.
- (44) Wever, F., and W. Schmidt
Structure of rolled metals of the face centered cubic
type. Z. Tech. Physik 8: 398-400. 1927.
- (45) Williams, C.
Thermal expansion and the ferromagnetic change in
volume of nickel. Phys. Rev. 46: 1011-1014. 1934.
- (46) Wilson, R. R.
A vacuum-tight sliding seal. Rev. Sci. Instr. 12:
91-93. 1941.